Taylor & Francis
Taylor & Francis Group

WALL PROPERTIES AND HEAT TRANSFER IN NEAR-WALL TURBULENT FLOW

Iztok Tiselj, Andrej Horvat, and Borut Mavko
Reactor Engineering Division, "Jožef Stefan" Institute, Ljubljana, Slovenia

Elena Pogrebnyak, Albert Mosyak, and Gad Hetsroni
Department of Mechanical Engineering, Technion—Israel Institute of Technology, Haifa, Israel

Direct numerical simulation of a passive scalar in fully developed turbulent channel flow is used to show that Nusselt number is not only a function of Reynolds and Prandtl number, but also depends on properties of a heating wall. Variable thickness of the heating wall and variable heater properties, combined in a fluid–solid thermal activity ratio $K = \sqrt{\rho_f c_{pf} \lambda_f / \rho_w c_{pw} \lambda_w}$, can change the Nusselt number of the turbulent channel flow for up to 1% at the same Reynolds and Prandtl number and at the same wall heat flux.

1. INTRODUCTION

Thermal conditions at a heating wall in contact with turbulent flow are known to be dependent on wall-side unsteady conduction. Such a conjugate heat transfer problem was studied by Polyakov [1], who demonstrated analytically that temperature fluctuations near a wall differ for different fluid–solid combinations. This finding was later confirmed experimentally by Iritani et al. [2], Khabakhpasheva [3], Hetsroni and Rozenblit [4], and Mosyak et al. [5]. Computational strategies applied to reveal the magnitude of temperature fluctuations at the fluid–solid interface are described by Kasagi et al. [6], who performed the analysis with a 2-D unsteady turbulent model. Later, Tiselj et al. [7] repeated the calculations with a more accurate direct numerical simulation (DNS).

The conjugate turbulent heat transfer near a heating wall depends on the wall thickness d_w and on the material properties of the wall and the fluid, which can be

NOMENCLATURE

a_1, a_2, b_1, b_2	coefficients of Taylor expansion	θ^+	dimensionless temperature (temperature difference)
c_p	specific heat at constant pressure	λ	thermal conductivity
d_w	heating wall thickness	ν	kinematic viscosity
K	thermal activity ratio $\left(= \sqrt{\rho_f c_{pf}\lambda_f / \rho_w c_{pw}\lambda_w}\right)$	ρ	density
		τ_w	time-averaged wall shear stress
Nu	Nusselt number $[= -(2\delta/\lambda)q_w/(\theta_B - \theta_w)]$	**Subscripts and Superscripts**	
Pr	Prandtl number $(= \rho c_p \nu/\lambda)$	$(\ )^+$	normalized by the wall variables, $u_\tau,\ \nu,\ T_\tau$
q_w	time-averaged wall heat flux	$(\ )_B$	bulk velocity or temperature
Re	Reynolds number	$(\ )_W$	value at the wall
Re$_\tau$	friction Reynolds number	$\langle\ \rangle_{x,y,z,t}$	averaging along the directions denoted in the subscripts
t	time	$(\ )'$	fluctuating part of the variable
T	temperature	$(\ )_N$	calculated with nonfluctuating wall temperature boundary condition
T_τ	friction temperature $(= q_w/\rho_f c_{pf}u_\tau)$		
u	velocity $[= (u, v, w)]$		
u_τ	friction velocity $\left(= \sqrt{\tau_w/\rho}\right)$	$(\ )_F$	calculated with fluctuating wall temperature boundary condition
x, y, z	streamwise, wall-normal, and spanwise coordinates		
δ	channel half-width or flume height		

expressed in a thermal activity ratio $K = \sqrt{\rho_f c_{pf}\lambda_f / \rho_w c_{pw}\lambda_w}$ (Kasagi et al. [6]). Based on values of K and d_w, two limiting cases of the conjugate turbulent heat transfer exist at the same Reynolds and Prandtl numbers and at the same wall heat flux [6, 7]:

1. The fluid–solid combination, where the thermal activity ratio tends to zero ($K = 0$) and the wall thickness remains larger than zero ($d_w > 0$), does not allow the turbulent temperature fluctuations in the fluid to enter the wall, i.e., the wall temperature does not fluctuate; this type of boundary condition is denoted as *nonfluctuating wall temperature boundary condition*.
2. The heating wall thickness d_w does not play a significant role in the infinite thermal activity ratio ($K = \infty$). In that case, wall temperature follows turbulent temperature fluctuations of the fluid, i.e., the temperature fluctuations induced by turbulence exist also inside the wall. This type of boundary condition is denoted as *fluctuating wall temperature boundary condition*.

The type of the actual thermal condition for a particular fluid–solid system with a given thermal activity ratio K and a heating wall thickness d_w is always somewhere between the two limiting cases and can be obtained from the studies of Kasagi et al. [6] and Tiselj et al. [7]. Both types of limiting boundary conditions were approached in the experimental work of Mosyak et al. [5]. They used a water flume heated with a thick copper plate ($K = 0.044$) for the nonfluctuating wall temperature case ($K = 0, d_w > 0$). For the $K = \infty$ case, they heated a water flume with a very thin (0.05-mm-thick) steel foil ($K = 0.12$). In experiments with air, the boundary condition is always very close to the nonfluctuating wall temperature case, due to small values of K ($\sim 10^{-3}$). A near-wall two-equation turbulence model was used by

Sommer et al. (1994) [8] to investigate validity and extent of the zero fluctuating wall temperature boundary condition $(K = 0)$ for heat transfer modeling and calculations. They concluded that the zero and the nonzero fluctuating wall temperature boundary conditions yield the same temperature distributions.

Although analytical derivations indicate the difference in the wall heat transfer due to the different values of the thermal activity ratio K and different heating wall thickness, the studies mentioned above [1–8] failed to identify the influence of the fluid and the solid properties on the heat transfer coefficient and the mean temperature field. Results of the studies [1–8] are, thus, in agreement with a simple relation found in most of the heat transfer textbooks (i.e., Kays and Crawford [9]):

$$\text{Nu} = f(\text{Re, Pr}) \tag{1}$$

Direct numerical simulation is an important tool for investigating near-wall turbulent heat transfer. In the past, results of the passive scalar field simulations in channel flow were obtained by Kasagi et al. [10], Kim and Moin [11], Kawamura et al. [12], Kasagi and Iida [13], and Na et al. [14]. Calculations presented in these articles were carried out for infinite channel flow with a uniform wall heating [10, 12, 13], isothermal walls [14], and volumetric heating of the fluid [11], all used nonfluctuating wall temperature boundary conditions. A similar DNS study of passive scalar transfer in the flume geometry, where the flow was limited with a single heating wall and a free surface, was performed by Tiselj et al. [15]. The study by Tiselj et al. [15] defined the thermal boundary conditions that correspond to the two limiting cases of conjugate turbulent heat transfer: the nonfluctuating wall temperature case $(K = 0, d_h > 0)$, and the fluctuating wall temperature case with $K = \infty$. Although different behavior of the turbulent temperature fluctuations in the diffusive sublayer was shown for both cases, the study [15] did not identify differences in the mean temperature profiles and heat transfer coefficients.

It is important to mention that the nonfluctuating and fluctuating wall temperature boundary conditions were denoted in [15] as "isothermal" and "isoflux boundary condition for the dimensionless temperature θ^+," respectively. This terminology is correct, but it was abandoned in the present work due to the possible confusion with the conventional meaning of the "isothermal" and "isoflux" boundary conditions, which were studied and compared, for example, by Kong et al. [16], Teitel and Antonia [17], Churchill [18], and Morinishi et al. [19]. In these works, the applied thermal boundary conditions were isothermal and isoflux boundary conditions, where each of them could be further divided into the fluctuating and nonfluctuating wall temperature boundary conditions. The nonfluctuating temperature boundary conditions were applied in [10–14, 17, 19], and both types of wall temperature fluctuations were applied in [15] and [16].

From the discussion above, it is clear that most methods used to solve the conjugate heat transfer problem have been based on turbulence phenomenological models or on DNS at low Reynolds numbers. In the present work, several direct numerical simulations at various Reynolds and Prandtl numbers have been performed with a modified version of the code used in [15]. Each DNS has been performed with a single velocity field and with two passive scalar fields, each for a different limiting type of thermal boundary condition at the fluid–solid boundary

using the same Prandtl number and the same wall heat flux. With reduced statistical uncertainty of this approach, we were able to demonstrate that the heat transfer rate of fully developed turbulent channel flow also depends on the properties of a heating wall:

$$Nu = f(Re, Pr, K, d_w) \tag{2}$$

As expected from the previous studies, which did not identify the influence of the wall properties, the variations of a heat transfer coefficient due to thermal activity ratio K and wall thickness d_w were small, less than 1% for all tested Prandtl and Reynolds numbers.

2. EQUATIONS AND BOUNDARY CONDITIONS

As the problem was well studied in the past, the governing equations of fully developed turbulent flow in an infinite channel or a flume and the scaling procedure can be found elsewhere [7, 9]. Temperature is assumed to be a passive scalar and does not affect the flow field. The dimensionless form (in wall units) of the energy equation in an infinite flume or a channel is given in a form that allows implementation of the equation in the pseudo-spectral DNS code:

$$\frac{\partial \theta^+}{\partial t^+} = -\nabla^+ \cdot \left(\mathbf{u}^+ \theta^+ \right) + \frac{1}{Pr} \nabla^{+^2} \theta^+ + \frac{1}{Re_\tau} \frac{u^+}{u_B^+} \tag{3}$$

The streamwise, the wall-normal, and the spanwise direction in Eq. (3) are denoted as x^+, y^+, and z^+, respectively. The dimensionless temperature θ^+ (also called "dimensionless temperature difference") is defined as

$$\theta^+(x, y, z, t) = \frac{\langle T_{WALL} \rangle_{t,z}(x) - T(x, y, z, t)}{T_\tau} \tag{4}$$

The averaging sign $\langle \cdot \rangle$ with subscripts t and z means ensemble averaging over the spanwise direction and time. The friction temperature is defined as $T_\tau = q_w / \rho_f c_{pf} u_\tau$ and the friction Reynolds number as $Re_\tau = u_\tau \delta / \nu$, where q_w is the time-averaged wall heat flux, u_τ is the friction velocity, and δ is the channel half-width or the flume height (δ in wall units is $\delta^+ = Re_\tau$). Term u^+/u_B^+ appears in Eq. (3) due to the transformation of the temperature T into the periodic variable θ^+, where the bulk streamwise velocity is defined as $u_B^+ = \langle u^+ \rangle_{t,x,y,z}$.

It is important to note that, due to the prescribed wall heat flux q_w, the averaged wall temperature $\langle T_{WALL} \rangle_{t,z}$ is increasing linearly in the streamwise direction x, and the averaged dimensionless temperature $\langle \theta^+ \rangle_{t,z}$ is not changing in the streamwise direction x.

Periodic boundary conditions are applied in the streamwise and the spanwise directions. The free-surface in the flume geometry is assumed to be free-slip and adiabatic. Definitions of the wall boundary conditions for the dimensionless temperature θ^+, which correspond to the two limiting cases of conjugate heat transfer, are defined by Tiselj et al. [15] as follows:

1. The nonfluctuating wall temperature boundary condition ($K = 0$ and $d_w > 0$) is defined in [15] as "the isothermal boundary condition for the temperature θ^+." It sets the temperature at the wall–fluid plane to zero:

$$\theta^+(x, y = y_{\mathrm{WALL}}, z, t) = 0 \tag{5}$$

This type of boundary condition was also used in previous DNS studies [10–14, 17, 19]. Again, the expression "isothermal boundary condition for the temperature θ^+" should not be mixed with the standard definition of the "isothermal boundary condition" used to denote the fixed temperature T on a given boundary. In our case, the physical temperature T on the channel wall is not constant, but is increasing linearly in the streamwise direction x.

2. The fluctuating wall temperature boundary condition ($K = \infty$) is defined in [15] as "the isoflux boundary condition for the temperature θ^+." In this case, the dimensionless temperature θ^+ is split in an averaged part $\langle\theta^+\rangle_{t,x,z}(y)$, which is constant, and a fluctuating part $\theta'^+(x, y, z, t)$. The boundary condition sets the averaged part at the wall to zero,

$$\langle\theta^+\rangle_{t,x,z}(y = y_{\mathrm{WALL}}) = 0 \tag{6}$$

whereas for the fluctuating part, the Neumann type of boundary condition is prescribed:

$$\frac{d\theta'^+}{dy}(x, y = y_{\mathrm{WALL}}, z, t) = 0 \tag{7}$$

Both types of limiting thermal boundary conditions can be consistent with isoflux or isothermal boundary conditions. Local wall heat flux is fluctuating for the nonfluctuating temperature boundary condition, while the wall heat flux is constant for the fluctuating wall temperature boundary condition. Numerical implementation of the fluctuating wall temperature boundary condition for θ^+ in the pseudo-spectral scheme that was used to perform the present DNS (Fourier series in streamwise and spanwise directions, Chebyshev polynomials in wall-normal direction) is fairly straightforward: the mean values of the temperatures at planes $y^+ = \mathrm{const}$ are given by the first terms of the corresponding Fourier expansions. Thus, Eq. (6) is used as a boundary condition for the differential equation for the mean part of the temperature field solved in the wall-normal direction, and Eq. (7) is used as a boundary condition for the higher wave numbers of the Fourier series. Details of the implementation of the fluctuating wall temperature boundary condition are given in [15].

3. HEAT TRANSFER RATE FOR THE FLUCTUATING AND NONFLUCTUATING WALL TEMPERATURE BOUNDARY CONDITIONS—THEORY

Despite the fact that none of the previous studies [5–8, 15] dealing with both types of the thermal boundary conditions revealed a difference in the heat transfer rate, it is possible to analytically prove the existence of different temperature profiles for the nonfluctuating and the fluctuating wall temperature boundary condition. For

fully developed channel or flume flow, the energy equation (3) is averaged in time from $t = 0$ to ∞, and in space from x and $z = -\infty$ to ∞. Further integration from $y^* = 0$ to y^+ (see also Kasagi et al. [10] or Kawamura et al. [12]) gives the following expression:

$$0 = -\langle v'^+\theta'^+\rangle_{t,x,z}(y^+) + \frac{1}{\mathrm{Pr}}\frac{d\langle\theta^+\rangle_{t,x,z}}{dy^+}(y^+) - 1 + \frac{1}{\mathrm{Re}_\tau u_B^+}\int_0^{y^+}\langle u^+\rangle_{t,x,z}(y^*)dy^* \quad (8)$$

Equation (8) shows that the mean temperature profile can be calculated if the mean velocity profile $\langle u^+\rangle_{t,x,z}$ and the wall-normal turbulent heat flux profile $\langle v'^+\theta'^+\rangle_{t,x,z}$ are known. It is known (Kawamura et al. [12]) that in the vicinity of the wall, the wall-normal turbulent heat flux for the nonfluctuating wall temperature boundary condition can be expanded in terms of y^+ as

$$\langle v'^+\theta'^+\rangle_{t,x,z}(y^+)_N = a_1 y^{+^3} a_2 y^{+^4} + \ldots \quad (9)$$

From the asymptotic behavior of v'^+ and θ'^+, a similar expansion can also be obtained for the fluctuating wall temperature boundary condition for θ^+ (see Kong et al. [16]):

$$\langle v'^+\theta'^+\rangle_{t,x,z}(y^+)_F = b_1 y^{+^2} + b_2 y^{+^3} + \ldots \quad (10)$$

As the near-wall behavior of the wall-normal turbulent heat flux depends on the thermal boundary condition, it is clear from Eq. (8) that the mean temperature profiles and the heat transfer coefficients also depend on the type of the thermal boundary condition. While the analytical calculation can prove the existence of the difference, it cannot give the magnitude of the differences, as the coefficients of the expansion terms in Eqs. (9) and (10) cannot be determined analytically. Moreover, the leading terms of the series in Eqs. (9) and (10) are not sufficient for accurate prediction of the difference in the temperature profiles for both types of boundary conditions.

4. HEAT TRANSFER RATE FOR THE FLUCTUATING AND NONFLUCTUATING WALL TEMPERATURE BOUNDARY CONDITIONS-DNS

The goal of the present study is to estimate the differences between the temperature profiles calculated with the nonfluctuating and fluctuating wall temperature thermal boundary conditions, which have not been reported yet. Table 1 contains the main results of the 12 various DNSs performed for different Reynolds and Prandtl number flows in the flume and the channel geometry. Test cases 1–6 were performed for the flume geometry, and test cases 7–12 for the channel geometry. They are denoted by F or C in the first column. The influence of the thermal boundary condition is limited to a conductive sublayer, whereas the differences between the channel and the flume geometry are limited to the zone near the center of the channel or the top of the flume. Some slight difference between the channel and the flume

Table 1. Summary of DNS calculations and main results

1	2	3	4	5	6	7	8	9	10	11	12	13	14	15
Case no.	Pr	Re_τ	Computational domain size (x^+, y^+, z^+)	Grid (x, y, z)	Time step	Averaging time	$(u_\tau - 1) * 10^2$	u_B^+	$((T_\tau)_N - 1) * 10^2$	ΔT_τ (%)	$(\theta_B^+)_N$	$\Delta\theta_B^+$ (%)	Nu_N	$\Delta\mathrm{Nu}$ (%)
1 F	5.4	170.8	$2146 \times 171 \times 537$	$256 \times 129 \times 128$	0.0256	2,562	−0.11	15.41	0.52	−0.11	45.77	0.36	40.47	−0.47
2 F	5.4	170.8	$2146 \times 171 \times 537$	$256 \times 129 \times 128$	0.0256	2,562	−0.58	15.46	0.28	−0.07	45.87	0.29	40.09	−0.36
3 F	5.4	424	$2664 \times 424 \times 1332$	$256 \times 129 \times 192$	0.0318	6,360	−0.70	17.64	−0.35	0.08	45.02	0.34	100.6	−0.26
4 F	1	170.8	$2146 \times 171 \times 537$	$128 \times 65 \times 72$	0.0512	5,124	−0.68	15.47	0.28	−0.01	16.98	0.99	20.04	−1.01
5 F	1	170.8	$2146 \times 171 \times 537$	$128 \times 65 \times 64$	0.0512	5,124	−0.12	15.41	−0.33	0.05	16.88	0.76	20.15	−0.71
6 F	1	170.8	$2146 \times 171 \times 537$	$128 \times 65 \times 64$	0.0512	5,124	−0.08	15.42	−0.27	−0.06	16.93	0.80	20.10	−0.87
7 C	1	170.8	$2146 \times 342 \times 537$	$128 \times 97 \times 64$	0.0854	6,832	0.10	15.48	0.04	−0.01	16.96	0.73	20.18	−0.74
8 C	0.71	150	$2356 \times 300 \times 942$	$128 \times 97 \times 128$	0.09	3,600	0.25	15.25	0.15	−0.06	13.82	0.83	15.47	−0.90
9 C	0.71	150	$4712 \times 300 \times 471$	$256 \times 97 \times 64$	0.09	9,000	−0.48	15.27	−0.11	−0.08	13.81	0.81	15.33	−0.90
10 C	0.71	150	$2356 \times 300 \times 471$	$128 \times 97 \times 64$	0.12	7,200	−0.18	15.22	0.02	−0.05	13.78	0.78	15.44	−0.83
11 C	0.71	150	$2356 \times 300 \times 942$	$192 \times 129 \times 160$	0.06	4,800	−0.05	15.23	−0.10	−0.01	13.78	0.78	15.44	−0.79
12 C	0.025	150	$2356 \times 300 \times 942$	$128 \times 97 \times 128$	0.09	4,500	0.49	15.25	−0.59	0.00	1.407	0.58	5.33	−0.58

DNS can be seen in the mean temperature profiles shown later in Figures 1c and 1d by comparing cases 6 and 7 in Table 1. These simulations were performed at the same Reynolds number Re$_\tau$ and at the same Prandtl number Pr, but for the different geometries. As can be seen in Figures 1c, 1d, and 2b, the near-wall behavior is not affected by differences in geometry.

Sizes of the computational domains (column 4 in Table 1), grid densities (column 5), time steps (column 6), and averaging times (column 7) are comparable with other similar DNS studies of Kasagi et al. [10], Kim and Moin [11], Kawamura et al. [12], and Na et al. [14], performed at similar Reynolds and Prandtl numbers.

In the previous DNS study of Tiselj et al. [15], the difference in the mean temperature profiles obtained with the two limiting types of fluid–solid thermal boundary conditions was attributed to statistical uncertainty. The results for each type of the boundary condition were obtained with separate code runs, which produced a slightly different velocity field. Statistical uncertainty of the velocity field is seen from the calculated values of the friction velocity u_τ in column 8 Table 1 [tabulated values are actually $100^*(u_\tau - 1)$] and the bulk velocity u_B^+ in column 9. Up to 0.7% variations of the calculated friction velocity from the expected value $u_\tau = 1$ are seen. The calculated friction velocity u_τ also gives the actual friction Reynolds number achieved in the simulation, which is compared to the friction Reynolds number Re$_\tau$ used in the equations (column 3 in Table 1): Re$_{\tau(CALC)}$ = Re$_\tau u_\tau$.

To reduce the sensitivity due to the statistical uncertainty, a modified computer code has been used in the present work. It allows simulations of multiple temperature fields with a single velocity field. This feature of the improved code eliminates the statistical uncertainty of the velocity term in Eq. (8) (last term on the right-hand side) and enables calculation of differences in the mean temperature profiles at the two limiting thermal boundary conditions, which remained hidden in the previous work of Tiselj et al.[15]. In the present work, DNS simulations with the fluctuating and nonfluctuating wall temperature boundary conditions were performed at friction Reynolds numbers Re$_\tau$ = 150, 170.8, and 424 (see Table 1). All DNS tests summarized in Table 1 were obtained with simultaneous DNS of a single velocity field and two thermal fields: one with the nonfluctuating and the other with the fluctuating wall temperature boundary condition. Four different Prandtl numbers were considered in this study: Pr = 5.4 (test cases 1–3), Pr = 1.0 (test cases 4–7), Pr = 0.71 (test cases 8–11), and Pr = 0.025 (test case 12).

While the statistical uncertainty of the velocity field has been eliminated for calculation of the heat transfer at various thermal boundary conditions, the statistical uncertainty of both temperature fields cannot be eliminated. Column 10 in Table 1 contains values of the calculated friction temperature $T_\tau = q_w / \rho_f c_{pf} u_\tau$ for the nonfluctuating wall temperature boundary condition [the tabulated quantity is actually $100^*(T_\tau - 1)$]. Compared to the expected value of $T_\tau = 1$, statistical variations of up to 0.5% can be observed. Slightly different values of T_τ are obtained for the fluctuating wall temperature boundary condition. However, instead of these values, the relative difference of the friction temperatures T_τ calculated for the both types of boundary conditions is given in the column 11:

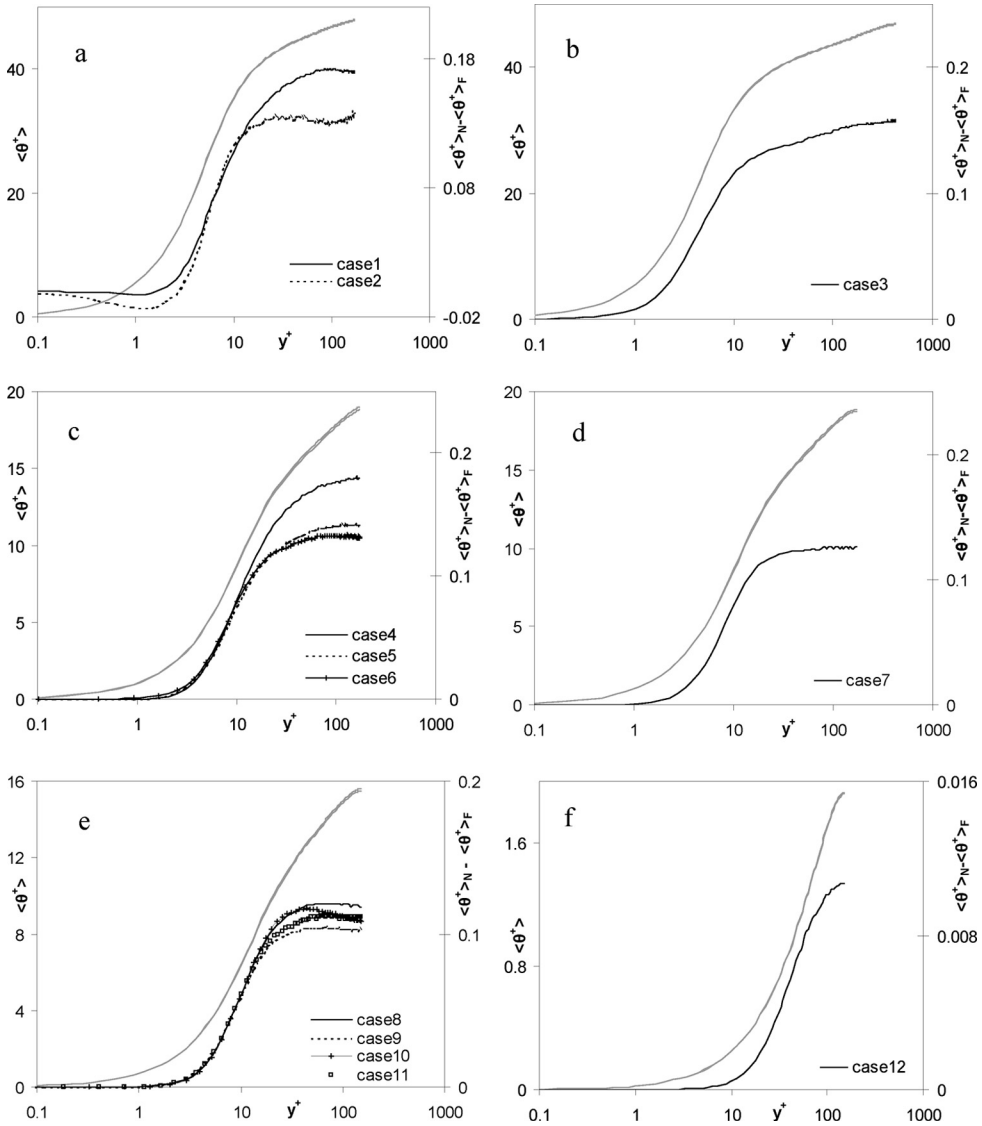$$\Delta T_\tau(\%) = 100 * \left[\frac{1 - (T_\tau)_F}{(T_\tau)_N} \right] \qquad (11)$$

Figure 1. Grey lines, left scale: two mean temperature profiles calculated with fluctuating and non-fluctuating wall temperature boundary conditions are too close to be resolved in graphs 1a, 1b, 1c, and 1f, while a small difference is visible in graphs 1c and 1e. Black lines, right scale: difference between the mean temperatures profiles calculated with nonfluctuating and fluctuating wall temperature boundary conditions. (*a*) $Re_\tau = 170.8$, $Pr = 5.4$ (cases 1, 2); (*b*) $Re_\tau = 424$, $Pr = 5.4$ (case 3); (*c*) $Pr = 1.0$ (cases 4–6), flume geometry; (*d*) $Pr = 1.0$ (case 7), channel geometry; (*e*) $Pr = 0.71$ (cases 8–11); (*f*) $Pr = 0.025$ (case 12).

As the friction temperature is proportional to the wall heat flux $T_\tau = q_w/\rho_f c_{pf} u_\tau$, the difference in Eq. (11) also means the difference of the wall heat flux for the both types of thermal boundary conditions, which directly affects the heat transfer coefficient. It can be seen in column 11 of Table 1 that relative differences of the friction

temperatures (and the heat fluxes) can be positive or negative, with absolute values smaller than 0.1%.

Column 12 in Table 1 gives the bulk temperatures in the channel or the flume calculated with the nonfluctuating wall temperature boundary condition for the dimensionless temperature θ^+:

$$\theta_B^+ = \frac{\langle u\theta \rangle_{x,y,z,t}}{u_B^+}$$

Column 13 shows the relative difference of the bulk temperatures calculated with the nonfluctuating and fluctuating wall temperature boundary condition for the dimensionless temperature θ^+:

$$\Delta\theta_B^+(\%) = 100 * \left[\frac{1 - (\theta_B^+)_F}{(\theta_B^+)_N} \right] \tag{13}$$

In all 12 simulations, the bulk temperature calculated with the nonfluctuating wall temperature boundary condition appears to be higher than the bulk temperature calculated with the fluctuating wall temperature boundary condition for the dimensionless temperature θ^+. Differences are between 0.3% and 1.0% and are significantly higher than the statistical uncertainties of the wall heat fluxes (and friction temperatures) in column 11 of Table 1.

Column 14 of Table 1 contains Nusselt numbers obtained from the numerical simulations performed,

$$\mathrm{Nu} = \frac{2\delta}{\lambda} \frac{q_w}{\theta_W - \theta_B} = 2\frac{(d\theta/dy)_W}{\theta_B} \tag{14}$$

column 15 shows the relative difference of the Nusselt numbers calculated with the nonfluctuating and fluctuating wall temperature boundary condition,

$$\Delta\mathrm{Nu}(\%) = 100 * \left(\frac{1 - \mathrm{Nu}_F}{\mathrm{Nu}_N} \right) \tag{15}$$

The numerical simulations performed show that heat transfer near the heating flat wall is between 0.3% and 1.0% more efficient when the fluctuating wall temperature boundary condition is imposed at the wall–fluid interface than in the case of the nonfluctuating wall temperature boundary condition for dimensionless temperature θ^+. As these differences are of the same order of magnitude as the statistical uncertainty of the previous study [15], it is clear why they have remained unnoticed.

Figure 1 presents mean temperature (θ^+) profiles at various Prandtl numbers (gray curves upper left in each figure, with corresponding temperature scale on the left). Only two temperature profiles are given in Figures 1a (case 1), 1c (case 6), and 1e (case 11), as the profiles of the other simulations are too close to be resolved on these figures. The very small differences between the temperature profiles calculated with fluctuating and nonfluctuating wall temperature boundary conditions are barely

visible in temperature profiles in Figure 1. A better view of the difference in the mean temperature profiles is given by the black lines in Figure 1 (right scale), where the mean temperature profile calculated with the fluctuating wall temperature boundary condition is subtracted from the mean temperature profile calculated with the nonfluctuating wall temperature boundary condition. It is clearly visible that the difference is accumulated in the near-wall diffusive layer and remains constant as the distance from the wall increases. Temperature differences in Figures 1 also give an impression of the statistical uncertainty. That is, the lowest statistical uncertainty is seen in Figure 1e at $Pr = 0.71$, where the largest computational domain and the longest averaging times were applied.

Figure 2 shows the wall-normal turbulent heat fluxes for each type of boundary condition. The differences are accumulated only in the conductive sublayer. The limiting near-wall behavior of the wall-normal heat fluxes is in agreement with the theoretical predictions of Eqs. (9) and (10) for the nonfluctuating and fluctuating wall temperature boundary condition for θ^+, respectively.

Test case 3 was performed at a higher friction Reynolds number, $Re_\tau = 424$. Kawamura et al. [12] reported relatively weak influence of the Reynolds number on the near-wall behavior of the turbulent heat transfer statistics (mean temperature, root mean-square fluctuations, and turbulent heat fluxes) in a turbulent channel. However, their study was limited to the nonfluctuating wall temperature boundary condition for θ^+. The results of test case 3 show that conclusions of Kawamura et al. [12] also remain valid for the fluctuating wall temperature boundary condition.
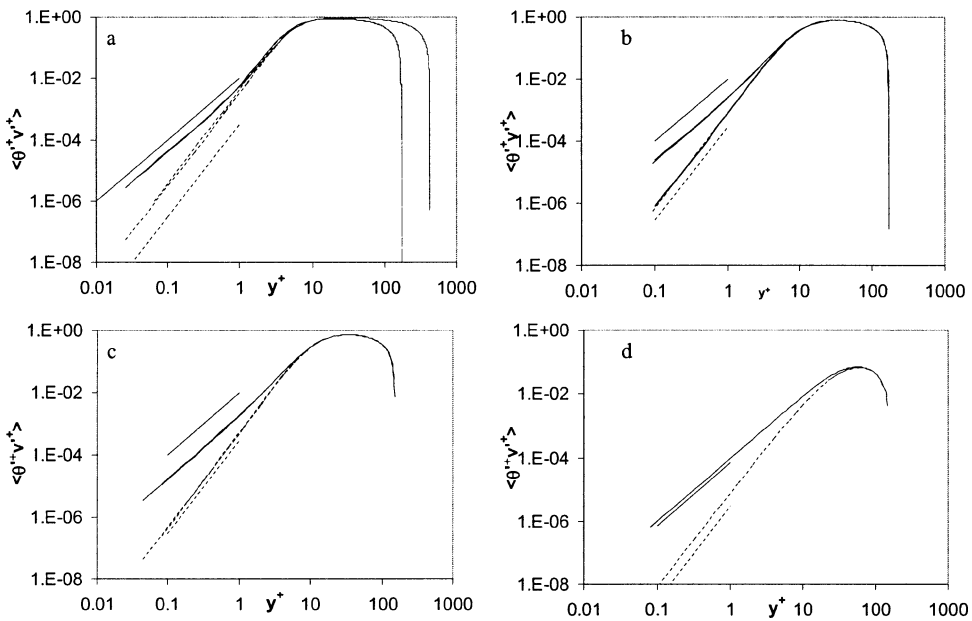

Figure 2. Mean wall-normal heat flux profiles at different Prandtl numbers, influence of the thermal boundary condition for temperature θ. Solid lines: fluctuating wall temperature boundary condition. Dashed lines: nonfluctuating wall temperature boundary condition. (a) $Pr = 5.4$ (cases 1–3); (b) $Pr = 1.0$ (cases 4–7); (c) $Pr = 0.71$ (cases 8–11); (d) $Pr = 0.025$ (case 12). Straight lines denote theoretical limiting behavior near the wall.

A very weak influence of the Reynolds number is seen in Table 1, which is of the same order as the statistical uncertainty and does not allow the conclusion that the difference in the Nusselt numbers depends on the Reynolds number.

Simulation 12 in Table 1 at Pr = 0.025 was performed for the relatively thick diffusive sublayer at very low Prandtl number. However, despite a wider diffusive sublayer, where the difference between the temperatures evaluated by the nonfluctuating and fluctuating wall temperature boundary conditions is generated, the difference between the corresponding Nusselt numbers remains the same as at higher Prandtl numbers.

The results of the DNS studies in Table 1 show that heat transfer rate depends on the properties of the heater. Nusselt number is slightly higher for fluid heated with the wall that allows the temperature fluctuations to propagate into the solid wall than for fluid heated with the wall that does not allow temperature fluctuations. The statistical uncertainty of the present results allows us to identify these differences, but it does not enable us to analyze these differences as a function of Reynolds and Prandtl numbers. Anyway, we assume that the same difference will also appear at larger Prandtl numbers [20].

Experimental confirmation of the results obtained in the present article is hardly possible with existing experimental setups, as the measurement errors of the fluid velocity, fluid temperature, and especially the heating power should be reduced below 1%. Although practical application of the results in the present work is not foreseen, it remains a remarkable feature that the material properties of the heated fluid boundaries actually affect the turbulent flow.

5. CONCLUSIONS

It is possible to show analytically the existence of the difference in heat transfer rates between the nonfluctuating and fluctuating wall temperature boundary conditions, which are applicable as the limiting types of the conjugate heat transfer boundary conditions in the fully developed turbulent flow near a heated wall. However, the magnitude of the difference cannot be calculated analytically. The present DNS results show up to 1% higher heat transfer rate for the fluid–solid combination with the thermal activity ratio $K = \infty$ (denoted in the present work also as the fluctuating wall temperature boundary condition) than for the other limiting case with thermal activity ratio $K = 0$ and finite heating wall thickness (denoted in the present work as the nonfluctuating wall temperature boundary condition). Although the results of this study are limited to the low friction Reynolds numbers $Re_\tau = 150, 170.8, 424$, and Prandtl numbers Pr = 0.025, 0.71, 1.0, 5.4, we assume that the same small differences in heat transfer, generated in the diffusive sublayer of the near-wall turbulent flow, also appear at other Reynolds and Prandtl numbers.

REFERENCES

1. A. F. Polyakov, Wall Effect of Temperature Fluctuations in the Viscous Sublayer, *Teplofizika Vysokih Temperatur*, vol. 12, pp. 328–337, 1974.
2. Y. Iritani, N. Kasagi, and M. Hizata, Heat Transfer Mechanism and Associated Turbulence Structure in the Near-Wall Region of a Turbulent Boundary Layer, *Proc. 4th Symp. on Turbulent Shear Flows*, Karlsruhe, Germany, 1985.

3. Y. M. Khabakhpasheva, Experimental Investigation of Turbulent Momentum and Heat Transfer in the Proximity of the Wall, *Heat Transfer 1986*, *Proc. 8th Int. Heat Transfer Conf.*, San Francisco, CA, USA, 1986.

4. G. Hetsroni, and R. Rozenblit, Heat Transfer to a Liquid-Solid Mixture in a Flume, *Int. J. Multiphase Flow*, vol. 20, pp. 671–689, 1994.

5. A. Mosyak, E. Pogrebnyak, and G. Hetsroni, Effect of Constant Heat Flux Boundary Condition on Wall Temperature Fluctuations, *Trans. ASME, J. Heat Transfer*, vol. 123, pp. 213–218, 2001.

6. N. Kasagi, A. Kuroda, and M. Hirata, Numerical Investigation of Near-Wall Turbulent Heat Transfer Taking into Account the Unsteady Heat Conduction in the Solid Wall, *Trans. ASME, J. Heat Transfer*, vol. 111, pp. 385–392, 1989.

7. I. Tiselj, R. Bergant, B. Mavko, I. Bajsic, and G. Hetsroni, DNS of Turbulent Heat Transfer in Channel Flow with Heat Conduction in the Solid Wall, *Trans. ASME, J. Heat Transfer*, vol. 123, pp. 849–857, 2001.

8. T. P. Sommer, R. M. C. So, and H. S. Zhang, Heat Transfer Modelling and the Assumption of Zero Wall Temperature Fluctuations, *Trans. ASME, J. Heat Transfer*, vol. 116, pp. 855–863, 1994.

9. W. M. Kays, and M. E. Crawford, *Convective Heat and Mass Transfer*, 2d ed., p. 259, McGraw-Hill, New York, 1980.

10. N. Kasagi, Y. Tomita, and A. Kuroda, Direct Numerical Simulation of Passive Scalar Field in a Turbulent Channel Flow, *Trans. ASME, J. Heat Transfer*, vol. 114, pp. 598–606, 1992.

11. J. Kim, and P. Moin, Transport of Passive Scalars in a Turbulent Channel Flow, in *Turbulent Shear Flows VI*, p. 85, Springer-Verlag, Berlin, 1989.

12. H. Kawamura, K. Ohsaka, H. Abe, and K. Yamamoto, DNS of Turbulent Heat Transfer in Channel Flow with Low to Medium-High Prandtl Number Fluid, *Int. J. Heat Fluid Flow*, vol. 19, pp. 482–491, 1998.

13. N. Kasagi, and O. Iida, Progress in Direct Numerical Simulation of Turbulent Heat Transfer, *Proc. 5th ASME/JSME Joint Thermal Engineering Conf.*, San Diego, CA, USA, 1999.

14. Y. Na, D. V. Papavassiliou, and T. J. Hanratty, Use of Direct Numerical Simulation to Study the Effect of Prandtl Number on Temperature Fields, *Int. J. Heat Fluid Flow*, vol. 20, pp. 187–195, 1999.

15. I. Tiselj, E. Pogrebnyak, C. Li, A. Mosyak, and G. Hetsroni, Effect of Wall Boundary Condition on Scalar Transfer in a Fully Developed Turbulent Flume, *Phys. Fluids*, vol. 13, pp. 1028–1039, 2001.

16. H. Kong, H. Choi, and J. S. Lee, Direct Numerical Simulation of Turbulent Thermal Boundary Layers, *Phys. Fluids*, vol. 12, pp. 2555–2568, 2000.

17. M. Teitel, and R. A. Antonia, Heat Transfer in Fully-Developed Turbulent Channel Flow—Comparison between Experiment and Direct Numerical Simulations, *Int. J. Heat Mass Transfer*, vol. 36, no. 6, pp. 1701–1706, 1993.

18. S. W. Churchill, A Reinterpretation of the Turbulent Prandtl Number, *Ind. Eng. Chem. Res.*, vol. 41, pp. 6393–6401, 2002.

19. Y. Morinishi, S. Tamano, and K. Nakabayashi, Direct Numerical Simulation of Compressible Turbulent Channel Flow between Adiabatic and Isothermal Walls, *J. Fluid Mech.*, vol. 502, pp. 273–308, 2004.

20. B. M. Mitrovic, and D. V. Papavassiliou, On the Prandtl or Schmidt Number Dependence of the Turbulent Heat or Mass Transfer Coefficient, *Chem. Eng. Sci.*, vol. 59, no. 3, pp. 543–555, 2004.